Effects of vertical velocity heterogeneity on stacking velocity and depth conversion

Ayman N. Qadrouh
KACST
aqadrouh@kacst.edu.sa

Andy Mitchell
The University of Adelaide
andy@asp.adelaide.edu.au

SUMMARY

Each layer of rock or sediment has its own velocity, that is, there are different velocities along the subsurface layers of the earth. Moreover, each layer has various values for different types of velocity. Therefore, the suggestion raised was to study the effects of vertical velocity heterogeneity on stacking velocity and depth conversion with different spread lengths, i.e., a small spread with a maximum offset of 2000 m and a large spread with a maximum offset of 4000 m. This study focused on the variation between stacking velocity and average velocity. In addition, the traveltime equation of Taner and Koehler (1969) for two terms and three terms was examined in order to find out which one provided better results.

Understanding the variations between the different types of velocities was crucial to this approach, which was carried out using data from the Tirrawarra-29 well in the Cooper Basin, South Australia. Well log data are used to calculate different types of velocities such as average velocity, root-mean-square velocity (for both short offset and three terms) and stacking velocity.

The results for both the $T-X$ plots and the T^2-X^2 plots for small (2000 m) and large spreads (4000 m) proved that the variation between average velocity and stacking velocity increases with offset. Furthermore, using the traveltime equation for three terms on the residual moveout plots for small and large offsets provided better results than using only two terms.

Key words: Stacking velocity, depth conversion and heterogeneity.

INTRODUCTION

Velocities usually vary with depth and the according horizontal subsurface layers of the earth. A mathematical equation is used to associate velocities with the arrival times of reflection events or with depth in order to understand the velocity variations. How the velocity is derived from the data is another factor in velocity variation. For instance, stacking velocities can be calculated from CMP gathers while average velocities are calculated from check shot data. Cordier (1985) has explained that the velocities in reflection seismology have an effect on two important factors of the interpreter's work. The first is the choice of velocities for the dynamic correction of sections. The second is the conversion of seismic times to depths. The relationship between average velocity and root-mean-square velocity was found by Al-Chalabi (1974) and he also explained that the difference between stacking velocity and root-mean-square velocity depends on tow elements which are heterogeneity factor and the spreading length. Bolshih (1965) extended the traveltimes function into a Taylor series of X^2. To obtain higher accuracy at far offset that should include the fourth order in the equation (Yilmaz, 2000).

The objective of this study is to determine the degree of deviation from a hyperbola of reflection traveltimes computed from a multi-layered velocity model representation of a real-world location. The accuracy of the moveout corrections and velocity information which can be obtained by fitting the various traveltime equations was investigated. The study was carried out using data from the Tirrawarra-29 well in the Cooper Basin. Two different maximum offsets were used in this study, a small offset of 2000m and a large offset of 4000m.

THEORY

We considered a multilayered medium composed of n^{th} layers, where each layer has its own thickness and velocity. Taner and Koehler (1969) derived the following equation for reflection traveltime in a multilayered medium:

$$T_x^2 = C_0 + C_1x^2 + C_2x^4 + C_3x^6 + \ ....$$

where x is the offset, and

$$C_0 = T_0^2$$

where T_0 is the two-way zero-offset traveltime

$$C_1 = \frac{1}{\mu_2}$$

$$C_2 = \frac{1}{4}\,\frac{\mu_2^2-\mu_4}{T_0^2\mu_2^4}$$

and

$$C_3 = \frac{2\mu_4^2-\mu_2\mu_6-\mu_2^2\mu_4}{T_0^4\mu_2^7}$$

with the following definitions of the terms

$$\mu_j = \frac{1}{T_0}\sum_{k=1}^{n} v_k^j t_0$$

$$\mu_2 = V_{rms}^2$$

$$V_{rms} = \left[\sum_{k=1}^{n} v_k^2 \; t_k \Big/ \sum_{k=1}^{n} t_k \right]^{1/2}$$

V_{rms} is the root-mean-square velocity, v_k is the velocity of the k_{th} layer, t_k is the two-way traveltime within the k_{th} layer, T_o is two-way vertical traveltime to the base of the n^{th} layer.

Al-Chalabi (1974) showed that the equation for the average velocity in a horizontally layered earth is:

$$V_a = \frac{2D}{T_0} = \frac{1}{T_0} \sum_{k=1}^{n} v_k t_k = \sum_{k=1}^{n} v_k t_k \Big/ \sum_{k=1}^{n} t_k$$

Dix (1955) showed that if the traveltimes and rms velocities to the top and base of the n^{th} layer in a model are known, then the interval velocity is given by:

$$V_{int}^2 = \frac{V_{rms}^2 t_n - V_{rms-1}^2 t_{n-1}}{t_n - t_{n-1}}$$

t_n is the zero offset arrival time for the base of the n^{th} layer.

The stacking velocity is obtained from the best-fit hyperbola to the measured reflection traveltimes in a common-midpoint gather. Essentially, it is the velocity required to duplicate the observed reflection traveltimes if the layered earth above the reflector was replaced by a single constant velocity layer. Hence the traveltime equation for a reflection in a multi-layered earth is approximated, in a least square means by:

$$T_x^2 = T_o^2 + \frac{X^2}{V_s^2}$$

where V_s is the stacking velocity.

Yilmaz (2000) has shown that the fourth-order moveout equation can be written as follows (by dropping the higher-order terms from Taner and Koehler's equation):

$$T_x^2 = T_0^2 + \frac{x^2}{V_{rms}^2} + C_2 x^4$$

This equation can also be approximated by the following time-shifted hyperbolic traveltime equation as shown by Yilmaz (2000):

$$T_x = T_0 \left(1 - \frac{1}{S}\right) + \sqrt{\left(\frac{T_0}{S}\right)^2 + \frac{x^2}{S V_{rms}^2}}$$

where S is a constant of the form

$$S = \frac{\mu_4}{\mu_2^2}$$

METHODOLOGY

Editing of data

There are two runs of sonic logs in Tirrawarra-29. The first sonic log was run from a depth of 113.84 m to 1639.06 m; the second run went from a depth of 1607.36 m to 2963.2 m. A number of editing has been made to these two sonic logs. Firstly, data in the first run below 1633.11 m were deleted as well as data above 1646.11 m in the second run. Secondly, a constant transit time 313.3 µs/m was inserted between 1633.11 m and 1646.22 m in order to produce a continuous velocity log. Thirdly, table 1 shows that the five nearest uphole surveys were used to fill in the missing velocities from the surface to the top of the first run. These solutions for generating velocity data at the top of the hole are not likely to be very accurate, but provide an approximation which is at least based on the available data as shown in figure 1. Fourthly, the edited sonic log was next check shot corrected, in order to make the times calculated in the model agree more closely with actual seismic times at the well. The check shot correction was achieved in two phases. In the first phase the drift is calculated. This gives the discrepancy between the times measured from check shot data and the sonic log. In the second phase a smoothed spline curve is fitted to the drift data, and this is used to calculate an adjustment to each sample of the sonic log, so that sonic times agree with the check shot times. Figure 2 illustrates the drift curve, and the initial sonic log (the red curve on the right) and the sonic log data after the correction (the black curve).

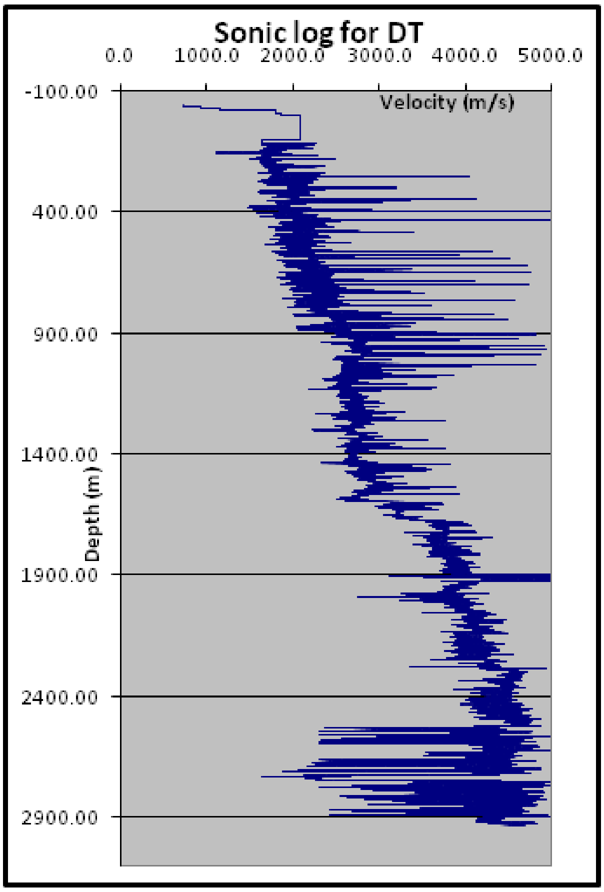

Fig. 1. Velocity model derived from sonic and uphole data. Depths measured from mean sea level.

Uphole survey number in PEPS database	Distance from Tirrawarra-29
22004	829 m
1885	835 m
1182	870 m
1878	919 m
2751	1036 m

Table 1. Distances of the five uphole surveys from Tirrawarra-29.

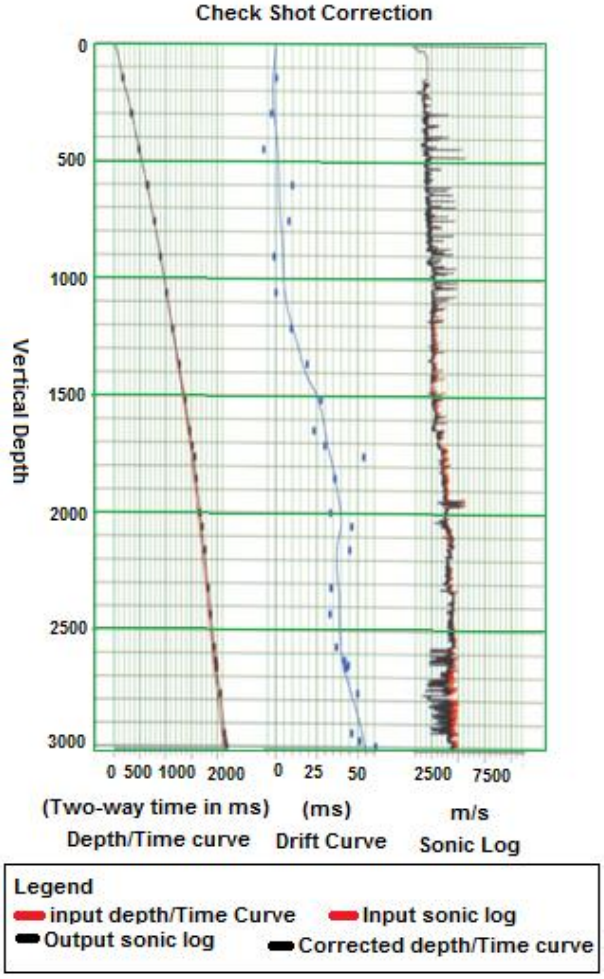

Fig. 2. Check shot Correction

Creating an S-wave log and a density log

The result of the procedure described above is a check shot-corrected P-wave velocity log. However, this is insufficient to create a synthetic CMP gather, which also requires an S-wave velocity log and a density log. It was therefore decided to calculate S-wave velocity log and a density log from the P wave velocity log by using Castagna's equation and Gardner's equation respectively as shown in Figure 3.

Creating a wavelet

A synthetic CMP gather, for which it requires a seismic wavelet to be specified. To avoid the real-life complications of interference between wavelets, and to be sure that the event traveltimes could be identified and measured from the synthetic gathers accurately, a very short and spike-like wavelet was required. The values of the bandpass wavelet parameters are shown in table 2. The wavelet itself is shown in figure 4. It consists of a central peak, only 2 msec wide, with negligible side lobes.

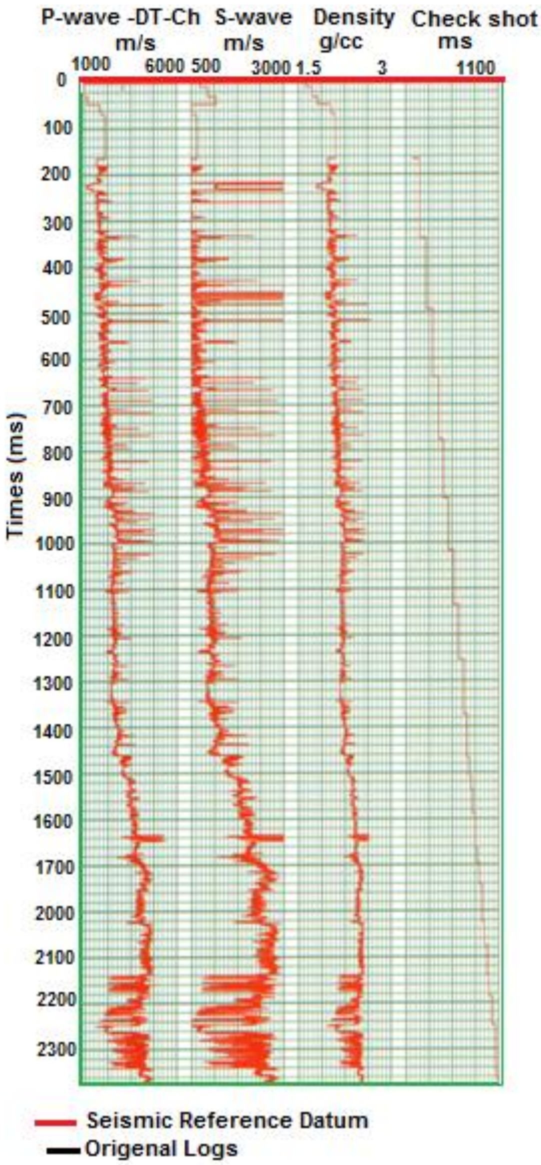

Fig. 3. Creating an S-wave velocity log and a density log from the P-wave velocity log.

Table 2. Values of bandpass wavelet parameters.

Bandpass wavelet parameters	Value
Low pass (Hz)	10
Low cut (Hz)	5
High pass (Hz)	60
High cut (Hz)	900
Wavelet length (ms)	20
Sample rate (ms)	0.5
Phase rotation	0

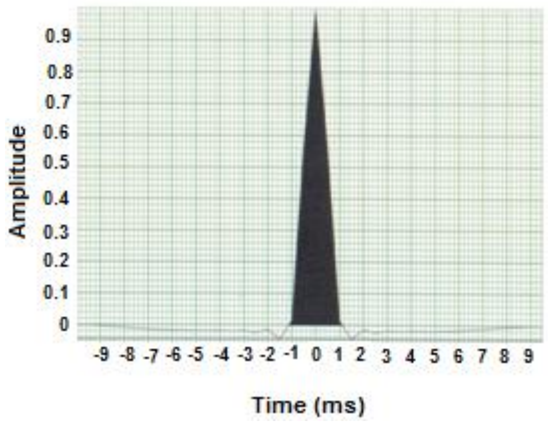

Fig. 4. Creating a wavelet

Creating a synthetic seismogram

The logs and wavelet were then used to calculate a synthetic CMP gather by using the Zoeppritz modelling. The synthetic seismogram was computed with 81 offsets, with the minimum and the maximum offset at 0 and 4000m respectively. This is based on the purpose of this study, which is to analyse the effect of different maximum offsets. The result is shown in figure 5.

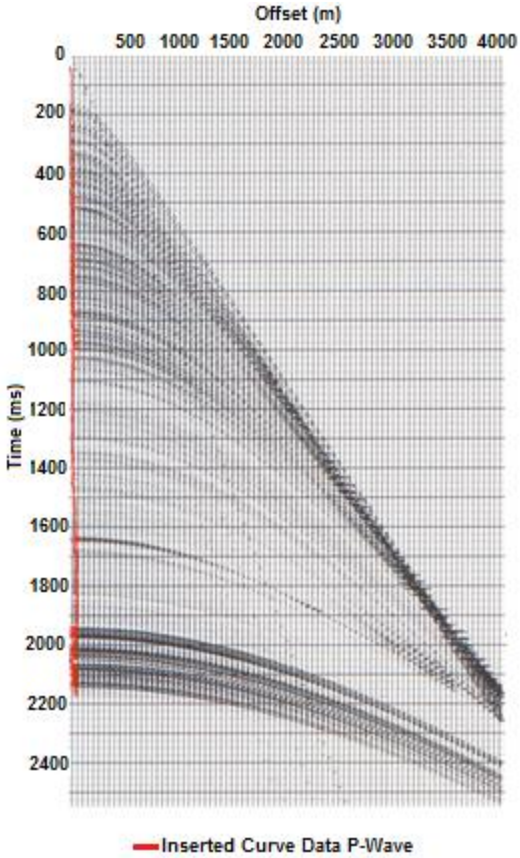

Fig. 5. Creating a synthetic seismogram

Picking horizons

For simplicity, it was decided instead to pick the traveltimes for selected events from the gather. Figure 6 shows the four reflections for which traveltimes were picked from the synthetic seismogram in this study. These reflections are generated by the marker horizons shown in table 3. The markers were chosen because they generate the characteristic reflections which are commonly mapped in the area, or are important reservoirs.

Table 3. The four horizons at particular depths.

Horizon	Depth (m)
Top Cadna-Owie Formation	1639.79
Top Toolachee Formation	2574
Top Patchawarra Formation	2771.21
Top Tirrawarra Formation	2941.66

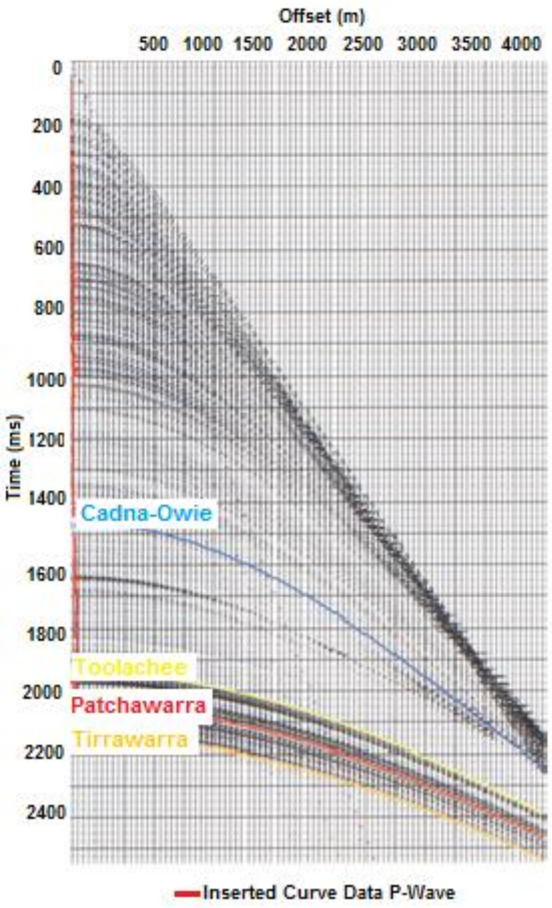

Fig. 6. Picking horizons

Model parameters

The synthetic gather was calculated from a velocity model. The exact values of T_0, V_a, V_{rms} and V_s can be calculated from the model. The resulting valuation of T_0, V_a, V_{rms} and V_s are for the four horizons are tabulated in tables 4and 5.

Parameters from traveltime analysis

The traveltimes picked for the synthetic gather for the four selected events were displayed for analysis. The traveltimes and offsets were displayed in a $T^2 - X^2$ plot. Linear regression of the data in this plot yields the parameters of the best fit hyperbola in $T - X$ plot. The slope of the line is $1/V_s$, from which an estimate of the stacking velocity can be obtained. It is assumed that this would be very similar to the stacking velocity obtained by picking a velocity spectrum computed from the synthetic gather. The intercept is T_0^2, and the value of T_0 calculated from this should be a good estimate of the time at which the event would appear if the event was NMO corrected with the calculated V_s value and then stacked.

A quadratic regression of the $T^2 - X^2$ data will yield the coefficients of the three-term approximation to the traveltime data. The constant term should give a better approximation to the true value of T_0 and the coefficient of X^2 should yield a more accurate estimate of V_{rms} than V_s derived from the linear regression.

After the velocities had been calculated from the parameters of the two regressions were calculated for the two and three term approximations for comparison with the picked traveltime data. In addition, traveltime data were also computed for the two term equation using the known values of V_a and V_{rms} instead of V_s, and also for the shifted hyperbola approximation, using the known values of T_0, V_{rms} and S.

Subtracting the calculated traveltimes from the picked traveltimes gives the residual moveout (RMO) which would remain if the event was NMO corrected using the corresponding travel time equation parameters. The RMO curves show how well corrected the event will be for the different equations, and thus how well the event will stack.

RESULTS

The analysis of the $T - X$ picks from each of the four interfaces measured from the synthetic gather for Tirrawarra-29 consists of three phases. The first phase is a $T - X$ graph. The second phase is a $T^2 - X^2$graph. The third phase is a residual moveout graph. Each phase can be divided into two parts; the first part analysed data between 0 to 4000m, and the second part used only data between offsets of 0 and 2000m. Note that the graphic results are presented here for only the 4000m spread for the Tirrawarra. This is due to the fact that the results of the studies for the other horizons were quite similar to those for the Tirrawarra event. The reason for only presenting the large spread is that the behaviour of the small spread can be recognised in the large spread plots.

The following is a discussion of the results represented in figures 7 to 9 and in tables 4 to 5. Three main conclusions can be drawn from these figures and tables.

1. $T - X$ plots calculated for different traveltime equations are hyperbolic (V_a, V_{rms}(short offset),V_s and shifted hyperbola) or almost so (V_{rms}(three term)) for both spreads. The curves for V_{rms}(three terms),V_s and shifted hyperbola are very similar, whereas the V_{rms}(short offset) curve gradually deviates from them at longer offsets.

   The observation can be made for the large offset and the small offset where average velocity obviously varies from other velocities as its variation increases with increased offset. The variation between different velocities in this study is the result of the calculation of average velocity values, which were smaller than other velocity values, i.e., V_s > V_{rms} (short offset and three terms) > V_a (as seen in tables 4 and 5). In other words, variations velocities' value were in the same horizon that caused the reduction in the curvature of reflection in the traveltime curves. As a result, performing the correction of NMO decreased because of increasing velocity and versa visa. Furthermore, the correction of NMO increased as increasing offsets.

2. Fitting different types of velocity (V_a, V_{rms}(short offset and three terms) and V_s) to $T^2 - X^2$ plots yields straight lines. For both large offset and small offset, the curves for V_s and V_{rms}(short offset) are quite the same at the beginning of the curve (for roughly the first four offsets from 81 offset), but when the number of the offset is increased, then gradually the values for both V_s and V_{rms}(short offset) start to differ. This result is due to the fact that the approximation of the stacking velocity value

is only equal to the values of the root-mean-square velocity for the short offset.

For the small spread, the V_s and V_{rms}(three terms) curves are quite the same from 0 to 2000 m. Because the calculation as seen in table 5 revealed small variations, however, these variations will appear when performing the large offset.

For both small and large spreads, the curves for both V_s and V_a gradually change when the offset is increased. The calculated values for the stacking velocity in this study were bigger than those for the average velocity as seen in tables 4 and 5.

3. The plots for the residual moveout values are obtained by fitting the traveltime equation by Taner and Koehler (1969) for two terms, three terms and time shifted hyperbola for both small and large spreads. The following observations can be made about the curves for the different velocities:

The time results for V_{rms} $(short\ offset\ and\ three\ terms\ )$ after NMO correction and shifted hyperbola after NMO correction are not affected by the different spread, because their calculations are not associated with the offsets.

The results for V_s after NMO correction are affected by spread length. The changing values of V_s after NMO correction is due to the computations directly depending on the offset. V_s after NMO correction the effect appeared in values starting at approximately –0.0003 sec with the small offset and at roughly –0.0018 sec with the large offset. This was supported by the calculations of time intercepts that show the values of T_0 $(\ 2\ terms)$ were increased with increased the offsets. Therefore, the values of V_s were increased with spread length as seen in tables 4 and 5.

The intercept times for V_{rms} (short offset and three terms) after NMO correction and shifted hyperbola after NMO correction started at $x = 0$ was $T_0\ = 0\ sec$, and then each curve had its own behaviour when the offsets increased. The curve for V_{rms} (three terms) after NMO correction, provided a better result than other curves, with values close to zero sec, which meant the curve for V_{rms} (three terms) after NMO correction appeared flatter. Both curves for shifted hyperbola after NMO correction and V_{rms} (short offset) after NMO correction provided good results up to roughly 1400 m and 750 m respectively, then they started to change gradually as long as the offsets increased. This meant NMO correction was valid for shifted hyperbola V_{rms} (short offset) for small offsets. On the other hand, the intercept time for V_s after NMO correction started at $x = 0$ was $T_0\ =- 0.0018$ sec. This meant NMO correction was invalid for V_s because T_0 started at -0.0018 sec, then moved downward to approximately 0.0019 sec. After that, the divergences started to move toward more or less -0.0037 sec.

CONCLUSIONS

The investigation of the variation of velocity in the vertical direction with different spread lengths was undertaken in this study, in particular the variation between stacking velocity and average velocity. The determination of this variation was the first objective of this thesis. Secondly, the traveltime equation by Taner and Koehler (1969) was inspected in order to find out whether the two-term or the three-term equation offers the better results.

The investigation of the well-log data resulted in the following findings: both the $T - X$ plots and the $T^2 - X^2$ plots for small and large spreads proved that the difference between average velocity and stacking velocity increases gradually with increasing offset. To conclude the findings, it became clear from the residual moveout plots that using the traveltime equation for three terms, provided better results than using only two terms for small and large offsets.

ACKNOWLEDGMENTS

The authors wish to thank KACST for financially support. The authors also would like to thank Dr. Dennis Cooke (Santos Ltd.) who generously sharing his knowledge and experience.

REFERENCES

Al-Chalabi, M 1974, *An Analysis of Stacking, RMS, Average, and Interval velocities over a Horizontally Layered Ground*: Geophysical Prospecting, vol. 22, pp. 458-475.

Bolshih, C., F., 1956, *Approximate model for the reflected wave traveltime curve in multilayered media:* Applied Geophysics, 15, 3-14 (in Russian).

Cordier, J. P 1985, *Velocities in Reflection Seismology*: D.Reidel Publishing Company, Dordrecht.

Dix, C. H., 1955, *Seismic velocities from surface measurements*: Geophysics, 20, 6886.

Taner. M. T & Koehler. F 1969, 'Velocity Spectra-Digital Computer Derivation and Applications of Velocity Functions', *Geophysics*, vol. 34, No. 6, pp.859-881.

Yilmaz, Öz 2000, *Seismic Data Analysis: Processing, Inversion and Interpretation of seismic data:* Society of Exploration Geophysicists, Tulsa.

Table 4. The results of different types of velocities and the intercept times for different terms for the four horizons (4000 m).

Horizon	Depth (m) *model*	T_0 (sec) *model*	T_0 (2 term) (sec)	T_0 (3 term) (sec)	V_a (m/sec) *model*	V_{rms} (m/sec) *model*	V_{rms} (short offset) (m/sec)	V_s (2 term) (m/sec)	V_{rms} (3 term) (m/sec)	S *model*
Cadna-Owie	1639.79	1.4625	1.467141	1.4613	2242.48	2286.3	2273	2325	2261	1.1366
Toolachee	2574	1.9403	1.942760047	1.9403	2653.21	2784.4	2845.09	2849	2774	1.4233
Patchawarra	2771.21	2.0483	2.050334	2.0484	2705.84	2815.6	2813.53	2896	2840	1.4228
Tirrawarra	2935.5	2.1415	2.143084	2.1415	2741.58	2878.7	2873.74	2929	2887	1.4054

Table 5. The results of different types of velocities and the intercept times for different terms for the four horizons (2000 m).

Horizon	Depth (m) *model*	T_0 (sec) *model*	T_0 (2 term) (sec)	T_0 (3 term) (sec)	V_a (m/sec) *model*	V_{rms} (m/sec) *model*	V_{rms} (short offset) (m/sec)	V_s (2 term) m/sec	V_{rms} (3 term) m/sec	S *model*
Cadna-Owie	1639.79	1.4625	1.462716	1.4625	2242.48	2286.3	2273	2290	2280	1.1366
Toolachee	2574	1.9403	1.940432632	1.9403	2653.21	2784.4	2845.09	2798	2781	1.4233
Patchawarra	2771.21	2.0483	2.048472	2.0483	2705.84	2815.6	2813.53	2851	2836	1.4228
Tirrawarra	2935.5	2.1415	2.141564	2.1415	2741.58	2878.7	2873.74	2889	2875	1.4054

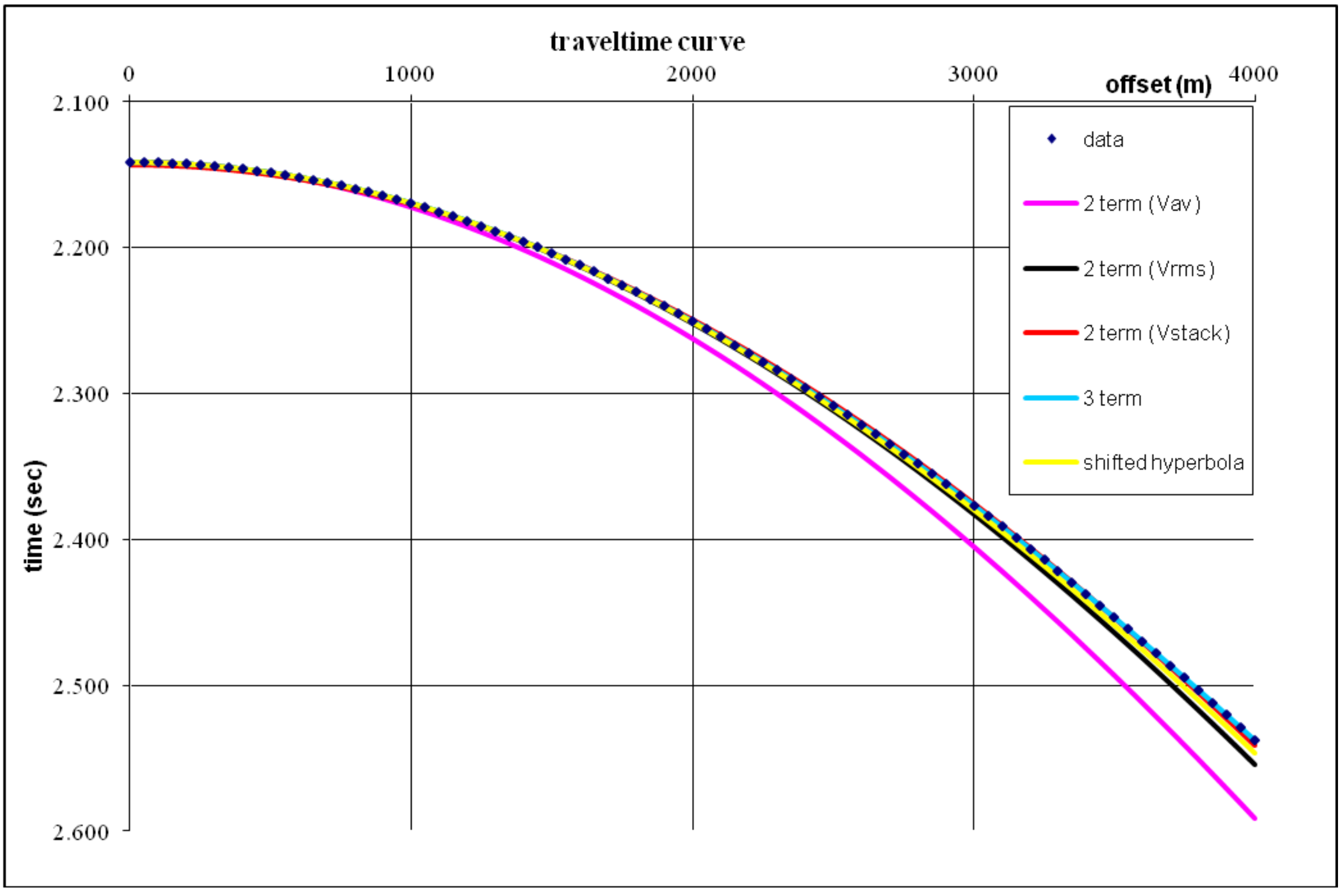

Fig. 7. $T-X$ plots calculated for different traveltime equations are hyperbolic (V_a, V_{rms}(short offset), V_s and shifted hyperbola) or almost so (V_{rms}(three term)) for 4000m.

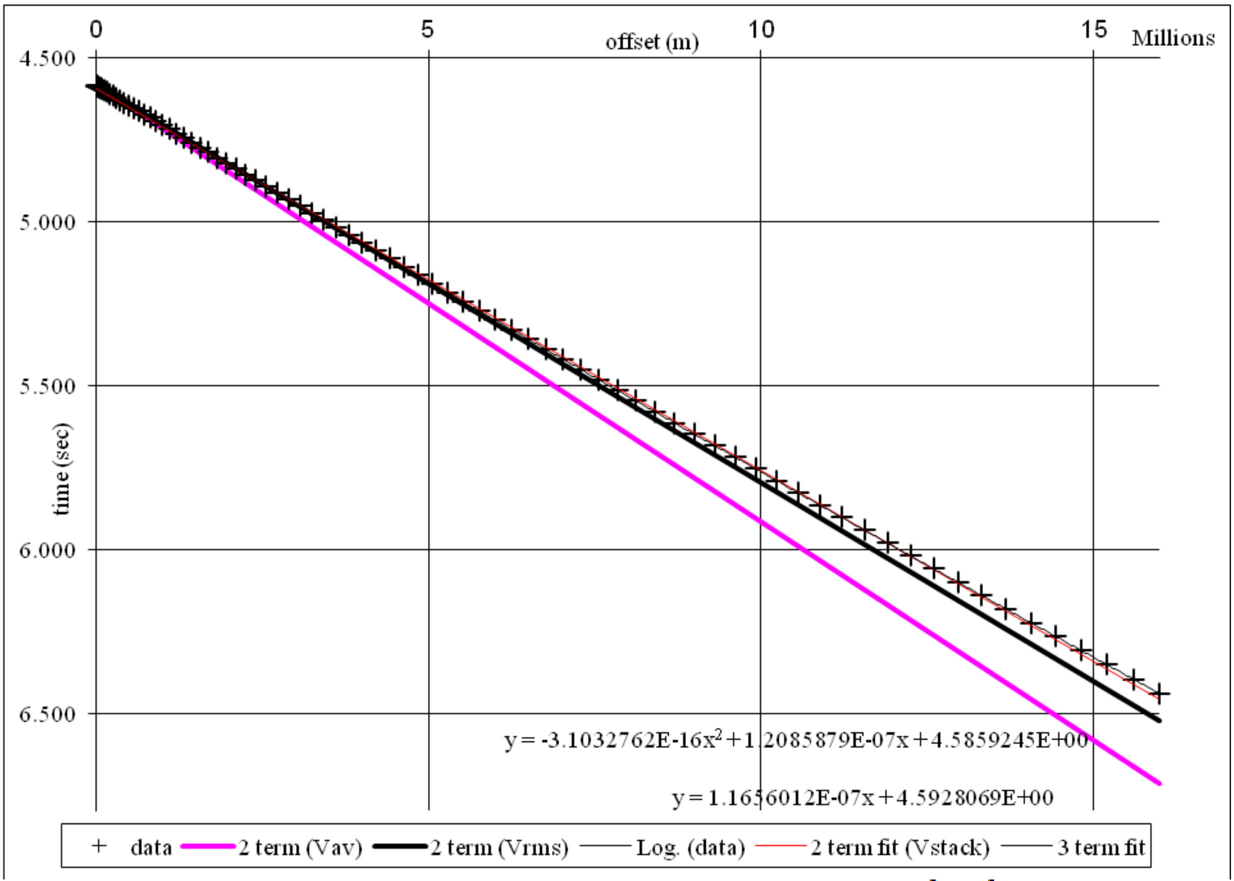

Fig. 8. Fitting different types of velocity $(V_a, V_{rms}$ (short offset and three terms) and V_s) **to** $T^2 - X^2$ **plots.**

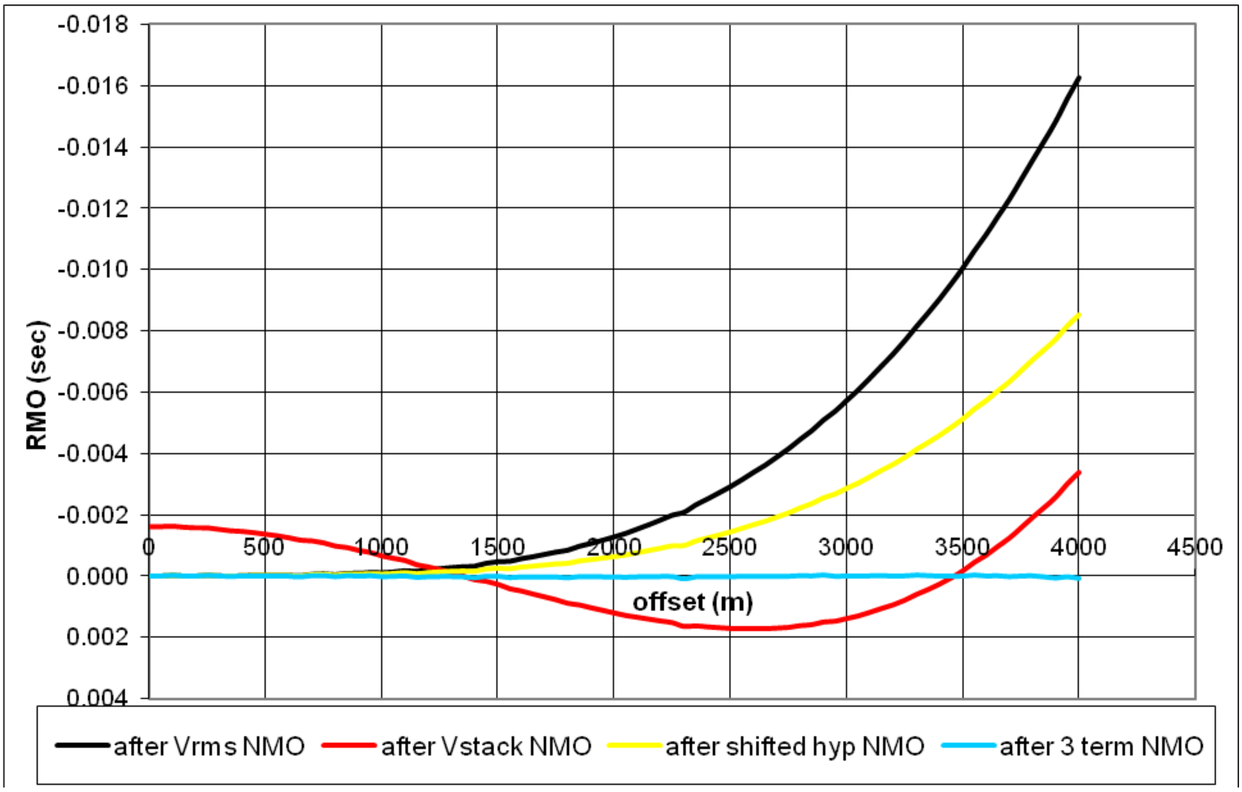

Fig. 9. The plots for the residual moveout values.